ISSN 1330-3651 (Print), ISSN 1848-6339 (Online)
Received: 23 October 2025; Accepted: 31 January 2026

https://doi.org/10.17559/TV-20251023003085
Original scientific paper

Modelling and Analysis of Wellbore Pressure Behaviour During Fixed-Valve Fishing in Thermal Recovery Wells

Zhuoran LI

Abstract: In fishing operations in thermal recovery wells, downhole throttle valves are often involved, altering the flow path of the injected fluid and leading to complex wellbore pressure interactions. To study these effects, this research established a coupled annulus-throttle valve-tubing flow model and conducted numerical simulations incorporating detailed valve geometry and turbulence characteristics. The results show that the pressure drop across the throttle valve is strongly dependent on flow rate and roughly proportional to the square of the injection rate. When the flow rate increases from 4 t/h to 10 t/h, the pressure drop rises from 1.00 MPa to 5.75 MPa, significantly increasing the required wellhead injection pressure. However, the influence of formation pressure is minimal; for every 2 MPa increase in formation pressure, the wellhead pressure changes by only 0.06 MPa. This coupled model elucidates the mechanism controlling the wellbore pressure distribution during fixed-valve fishing, providing a quantitative basis for selecting injection parameters and ensuring operational safety in thermal recovery wells.

Keywords: diversion effect; fishing technology; throttle valve; wellbore pressure drop

1 INTRODUCTION

In the thermal recovery process of heavy oil, fishing operations for downhole fixed valves are critical technical steps for maintaining wellbore integrity and restoring production capacity [1-3]. Unlike conventional fishing techniques, when a multi-orifice throttle valve is installed in the bottom hole annulus, the flow path of the fishing fluid is fundamentally altered: one portion enters the tubing to push the fixed valve upward, while another portion diverts into the formation through the throttle orifices. This forms a complex piping system involving valve pressure drop, transient flow diversion, and annulus-tubing coupling [4-7]. This diversion effect results in a strongly nonlinear characteristic of the wellbore pressure distribution, making accurate prediction and control of the wellbore pressure during the operation a core challenge for ensuring operational safety and efficiency.

Research on wellbore multiphase flow and throttle valve characteristics has laid a foundation for understanding complex wellbore flows. In the theoretical study of wellbore multiphase flow, research has extended from conventional conditions to complex operating scenarios. For instance, in the dynamic well killing process of complex-structure wells, Yang et al. [8] revealed the dynamic influence patterns of initial gas influx, well-killing fluid parameters, and wellbore trajectory on wellbore pressure. Regarding natural gas hydrate extraction, Ouyang et al. [9] established a fully transient non-isothermal gas-liquid-solid multiphase flow model, successfully characterizing the coupling mechanism between hydrate decomposition phase change and wellbore multiphase flow. Furthermore, research by Yin et al. [10] on wellbore multiphase transient flow during drilling in deepwater shallow hydrate reservoirs has further enriched the theoretical understanding of flow under extreme environments. Recent progress has also been made in coupled wellbore-reservoir modeling. Jafari Raad et al. [17] investigated wellbore dynamics during CO_2 injection using a non-isothermal transient model, revealing the impact of gas-liquid transient flow and phase change on bottomhole pressure; Chauhan et al. [18] conducted a computational study on two-phase flashing flow in geothermal wellbores affected by calcite scaling. Abdelaaland Zeidouni [19] further utilized a coupled model to evaluate CO_2 injection rate distribution over thick multilayer storage zones, emphasizing the controlling roles of gravity and flow capacity on rate allocation.

In the study of throttle valve characteristics, to achieve high-precision pressure control, Chen et al. [11] optimized the variable-diameter profile of the throttle valve, establishing a dynamic mapping relationship between stroke and throttling area, which significantly improved the linear response characteristics between opening and pressure drop. Addressing the erosion issue of throttle valves in ultra-deep high-pressure gas wells, Du et al. [12] clarified the erosion rate distribution and throttling temperature variation patterns through numerical simulation. Meanwhile, studies by Qu et al. [13] indicate that enhancing the performance of micro-flow control valves through structural improvements and parameter optimization is also an important current research direction. In model development, Leporini et al. [20] improved a multiphase flow model for wellhead chokes under both critical and subcritical conditions using field data. Gabel et al. [21] employed a combined experimental and computational approach to deeply investigate the complex vortex structure and flow-induced vibration mechanisms of incompressible flow inside choke valves. For specific field applications, Tellache et al. [22] developed improved multiphase flow choke models for the Algerian HMD oil field, effectively enhancing production rate prediction accuracy.

In the interdisciplinary field of numerical simulation, complex flow, and intelligent algorithms, models and methods are continuously developing toward refinement and intelligence. Deng et al. [14] established a full-wellbore complex flow mathematical model based on the drift-flux model, capable of simulating pressure evolution under complex conditions with high accuracy. The fishing practices for complex debris in shale gas horizontal wells by Feng et al. [15] provide engineering insights for handling downhole flow obstacles. Related simulation studies have also extended to solid-liquid two-phase flow in the annulus of fishbone-shaped multilateral horizontal wells to optimize wellbore cleaning [16]. Furthermore, machine learning methods are being widely applied to flow prediction and optimization. Alakbari et al. [23] developed

a robust model based on an Adaptive Neuro-Fuzzy Inference System (ANFIS) for accurately predicting pressure drop in vertical multiphase flow. Akbari et al. [24] applied algorithms such as Multilayer Perceptron (MLP) to optimize wellhead choke flow for predicting well performance parameters. Nazari et al. [25] explored the use of Physics-Informed Neural Networks (PINNs) to model mass flow rate in production wellbores, offering a new approach to integrate physical principles with data-driven modeling.

However, despite significant progress in the aforementioned research, clear model inapplicabilities persist when applied to the specific operational scenario of downhole fixed valve fishing. Firstly, most existing models are constructed based on specific flow conditions, and their applicability becomes limited when applied to the transient flow with continuously varying injection rates and boundary conditions during fishing operations [26]. More importantly, existing literature lacks a detailed description of the specific mechanism of the throttle valve within the complex wellbore system, particularly how its internal flow structure affects and couples with the overall pressure distribution of the annulus and tubing [27]. This makes it difficult to accurately predict the decisive impact of throttle valve diversion on the wellhead operating pressure, a critical safety parameter. Therefore, developing a dedicated coupled model capable of organically integrating annulus pipe flow, the internal nonlinear flow of the throttle valve and tubing pipe flow is crucial for understanding and controlling the wellbore pressure dynamics during fishing operations.

To address this research gap, this study aims to establish a coupled flow mathematical model specifically for the annulus-throttle valve-tubing system to accurately reveal the variation patterns of wellbore pressure during fishing operations. The core feature of this model lies in its focus not only on coupling the flow equations of each sub-region but also on characterizing the dynamic pressure drop characteristics of the throttle valve as a key flow-diverting element and its interaction with the system pressure field. Compared to general models, this research aims to elucidate the specific composition and dominant influencing factors of wellhead pressure under this particular operational configuration, especially quantifying the relative contributions of the throttle valve diversion effect and formation pressure changes to the wellhead pressure, providing field operators with direct theoretical guidance on how to precisely control wellhead pressure by adjusting operational parameters, thereby enabling the safety optimization of fixed valve fishing operations.

2 METHODS

2.1 Mathematical Model Development

During fixed valve fishing operations, the fishing fluid is injected through the tubing-casing annulus and flows downward along the annular space to the bottomhole. At the bottomhole, the fluid passes through three Φ3.3 mm orifices, generating a pressure drop. One portion of the fluid enters the formation through the orifices, resulting in fluid loss, while the other portion enters the tubing to push the fixed valve upward. Under the continuous action of fluid injection, the fixed valve moves upward until it is successfully retrieved at the wellhead. A schematic diagram of the fixed valve fishing process is shown in Fig. 1.

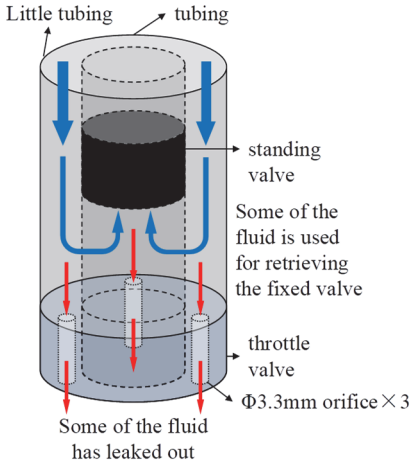

Figure 1 Schematic diagram of the fixed valve fishing process

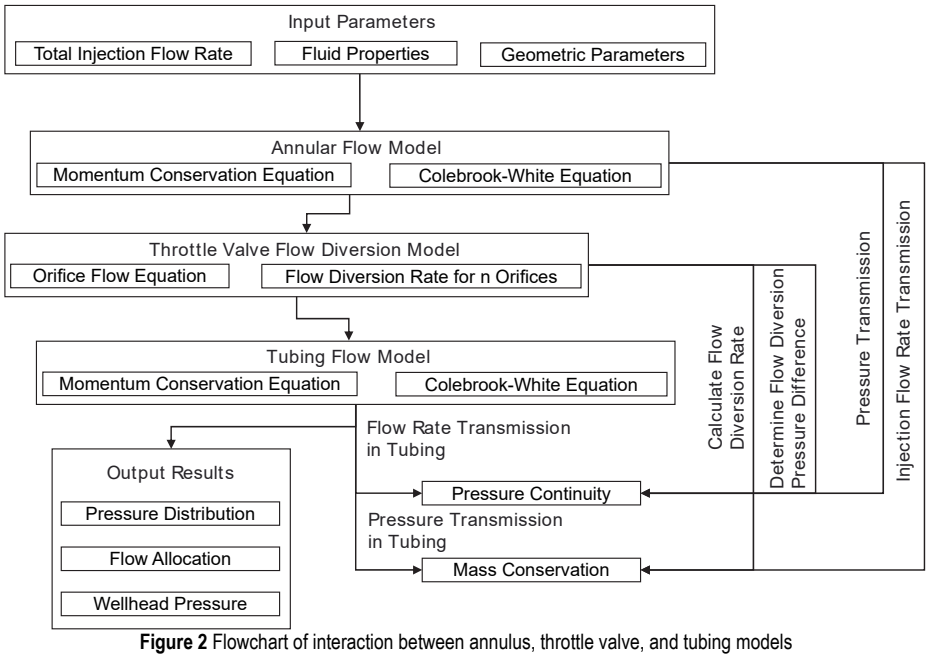

Figure 2 Flowchart of interaction between annulus, throttle valve, and tubing models

To investigate the distribution characteristics of wellbore pressure during the fixed valve fishing process, a mathematical model for wellbore pressure drop is established, considering the flow diversion and pressure drop effects of the throttle valve. The model consists of three components: the annular pressure drop model, the throttle valve pressure drop and flow diversion model, and the tubing string pressure drop model. Meanwhile, this study proposes the following core assumptions based on the operational characteristics:

(1) Single-phase incompressible flow: The fishing fluid is a Newtonian fluid with constant density and viscosity.

(2) Quasi-steady flow: Due to the slow progress of the fishing operation, transient flow is treated as a series of quasi-steady processes.

(3) Isothermal process: Heat exchange and temperature variations in the wellbore are neglected.

(4) Darcy flow for formation seepage: The flow diverted into the formation through the throttle valve orifices follows Darcy's law.

Since the model consists of three sub-models coupled through mass conservation and pressure continuity conditions, Fig. 2 illustrates the overall structure of the model and the logical relationships among the variables.

2.1.1 Annular Pressure Drop Model

The flow of the fishing fluid in the annulus satisfies the momentum conservation equation. The pressure drop is primarily composed of gravitational and frictional pressure drops:

$$\frac{dp_a}{dz} = \rho g \cos\theta + \frac{f_a \rho v_a^2}{2D_{h,a}} \tag{1}$$

included among these:

$$D_{h,a} = D_c - D_o \tag{2}$$

The annular friction factor f_a is calculated using the Colebrook-White equation:

$$\frac{1}{\sqrt{f_a}} = -2\log\left(\frac{\epsilon / D_{h,a}}{3.7} + \frac{2.51}{\mathrm{Re}\sqrt{f_a}}\right) \tag{3}$$

2.1.2 Throttle Valve Pressure Drop and Flow Diversion Model

The flow at the throttle valve satisfies the orifice flow equation. The flow rate through a single orifice is given by:

$$q_{\text{orifice}} = C_d A_o \sqrt{\frac{2\Delta p_v}{\rho}} \tag{4}$$

For a throttle valve within identical orifices, the total diverted flow rate is given by:

$$Q_{\text{loss}} = n \cdot q_{\text{orifice}} = n C_d A_o \sqrt{\frac{2\Delta p_v}{\rho}} \tag{5}$$

Therefore, the pressure drop across the throttle valve can be expressed as:

$$\Delta p_v = \frac{\rho}{2}\left(\frac{Q_{\text{loss}}}{n C_d A_o}\right)^2 \tag{6}$$

In the automotive, computer, and electronics industries, many companies have successfully practiced the mass customization model. For example, customers of Land Rover Motors, one of the most successful examples of mass customization, can collaborate with design teams to customize their cars, as can companies such as Dell and Hewlett-Packard in the computer industry and General Electric in the healthcare industry [7, 8]. Dell allows customers to personalize their products to their liking by configuring their PCs online and can deliver the final product quickly [9]. This practice of MC has received a positive response from both consumers and businesses. What makes these MC practices particularly effective is their precise alignment with individual user preferences - a factor that significantly enhances customer satisfaction. This alignment does not merely fulfill surface-level expectations; instead, it fosters a more profound sense of brand trust and emotional engagement. As a result, businesses benefit from stronger customer loyalty, which ultimately translates into measurable growth in product sales [10].

2.1.3 Tubing String Pressure Drop Model

The pressure drop in the tubing string includes gravitational and frictional pressure losses:

$$\frac{dp_t}{dz} = \rho g \cos\theta + \frac{f_t \rho v_t^2}{2D_{i,t}} \tag{7}$$

2.1.4 Model Coupling and Solution

The annular pressure drop model, the throttle valve pressure drop and diversion model, and the tubing string pressure drop model are coupled through mass conservation and pressure continuity:

Mass Conservation: The total injection flow rate at the annular inlet equals the sum of the flow rate diverted into the formation and the flow rate entering the tubing at the throttle valve:

$$Q_{\text{inj}} = Q_{\text{a}} = Q_{\text{loss}} + Q_{\text{tubing}} \tag{8}$$

Pressure Continuity: At the throttle valve location, the annular pressure minus the valve pressure drop equals the tubing inlet pressure:

$$p_a(L) = p_t(L) + \Delta p_v \tag{9}$$

Given the total injection flow rate and the system geometric parameters, the system of Eqs. (1) to (9) can be solved to determine the pressure distribution and the diverted flow rate.

2.2 Numerical Model Development

2.2.1 Geometric Modeling of Throttle Valve Pressure Drop Considering Precise Geometric Configuration

To achieve multi-scale flow simulation from local to system levels, this paper establishes two complementary geometric models, including:

1) Detailed 3D Model of the Throttle Valve: Based on the actual valve structure (Fig. 3), its internal complex fluid domain is extracted. The flow path is characterized as follows: three inlet throttle orifices of $\Phi 3.3 \times 12$ mm → a sudden-expansion annular chamber of $\Phi 20 \times 9$ mm → an outlet orifice of $\Phi 6 \times 5$ mm. This geometry is used to study fine flow phenomena within the valve, such as local jet flow, vortices, and pressure recovery.

2) Coupled Annular-Throttle Valve-Tubing System Model: To simulate the pressure response of the entire wellbore, a multi-scale coupled model integrating one-dimensional wellbore components with the three-dimensional throttle valve element is established (Fig. 4). At the same time, schematic diagrams of the dynamic flow processes in the annular and tubing sections are presented in Fig. 5. Here, the throttle valve is embedded as a three-dimensional subdomain within the system, and data exchange with the one-dimensional flow channels is conducted through coupling interfaces.

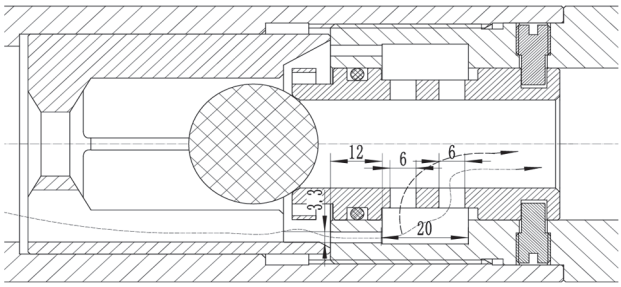

Figure 3 Specific geometric structure of the throttle valve

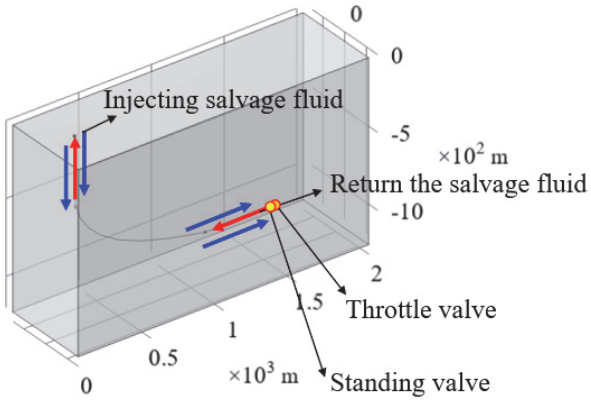

Figure 4 Geometric model of coupled annular-throttle valve-tubing flow

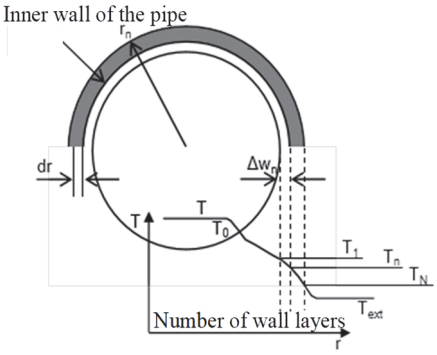

(a) Dynamic flow characteristics in tubing

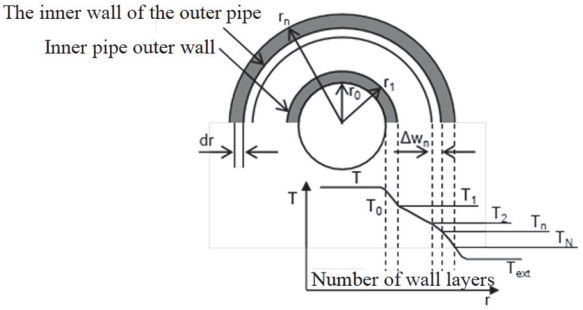

(b) Dynamic flow characteristics in annulus

Figure 5 Schematic diagram of dynamic processes in annular flow and tubing flow

2.2.2 Mesh Generation

For the two aforementioned geometries, different meshing strategies are adopted:

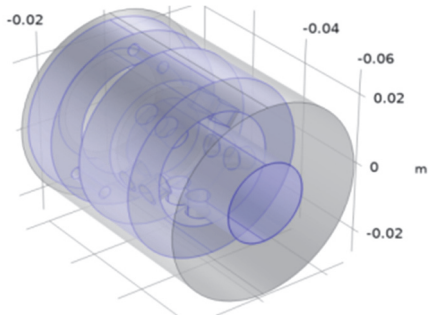

(a) Geometric configuration and internal fluid domain of the throttle valve

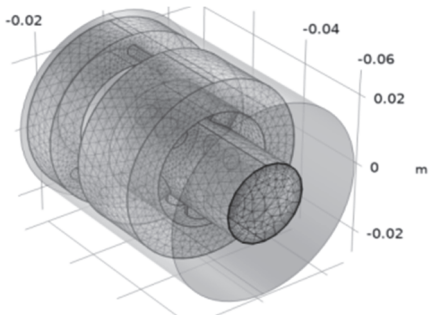

(b) Internal fluid domain grid division

Figure 6 Geometric structure of the throttle valve

1) Mesh for the detailed throttle valve model: Unstructured tetrahedral meshes are used (Fig. 6b), with local refinement applied in regions of high flow gradients, such as the orifices and walls.

2) Mesh for the system-coupled model: The annulus and tubing are discretized using one-dimensional pipe elements; the throttle valve region employs a three-dimensional mesh consistent with the detailed model but

appropriately simplified. At the coupling interfaces, conservation of mesh flux and physical quantity interpolation is ensured.

2.2.3 Boundary Conditions and Solver Settings

Inlet: Set as a mass-flow inlet, corresponding to the different operational injection flow rates

Outlet: Set as a static-pressure outlet.

Walls: Adopt a no-slip boundary condition, with near-wall treatment using standard wall functions.

A pressure-based coupled solver is selected, and all spatial discretization schemes employ the second-order upwind scheme to improve accuracy. The computation iterates until all residuals drop below 10^{-4} and key monitoring points stabilize.

2.2.4 Model Validation and Simulation Parameters

Well X in Block X is a horizontal well with a depth of 2019 meters. The fixed valve and throttle valve are located at the bottom of the well. The throttle valve has three throttle holes with a diameter of 3.3 mm. The insulated tubing has an inner diameter of 76 mm, while the small tubing has an outer diameter of 48.25 mm and an inner diameter of 40.89 mm. During the initial fishing operation, no throttle valve was found at the bottom of the well. At this time, the injection rate at the wellhead was 5 t/h, the return flow pressure at the wellhead was 4.2 MPa, and the injection pressure at the wellhead was 5 MPa. Tab. 1 shows the parameters used for simulation and model validation.

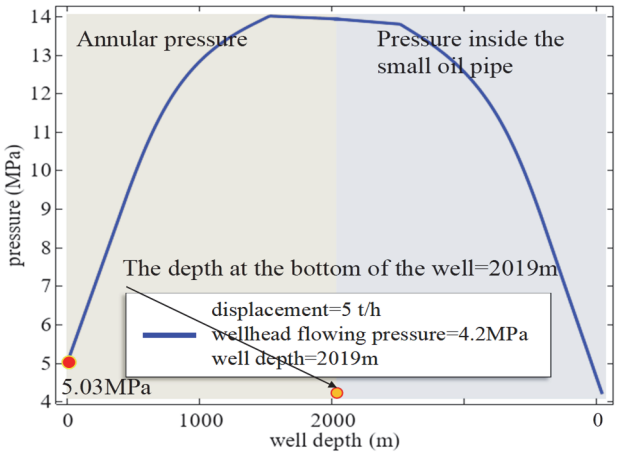

Figure 7 Pressure distribution in the wellbore and wellhead pressure results during the initial fishing operation without a throttle valve in Well X, Block X

Fig. 7 shows the wellbore pressure distribution without a throttle valve in Well X of Block X. As can be seen from the figure, when the wellhead return flow pressure is 4.2 MPa, the simulated wellhead injection pressure is 5.03 MPa, which is essentially consistent with the actual value of 5 MPa, with an error of 0.6%. This verifies the accuracy of the model and ensures the reliability of the numerical simulation.

Table 1 Simulation parameters

Parameter	Physical Interpretation	Unit	Value for Model Validation	Value for Parametric Analysis
ρ	Fluid density	kg/m³	1000	1000
μ	Fluid dynamic viscosity	mPa·s	0.798	0.798
Q_{inj}	Wellhead injection rate	m³/h	5	4, 6, 8, 10
$D_{h,a}$	Annulus diameter	mm	35.11	35.11
$D_{i,t}$	Tubing inner diameter	mm	40.89	40.89
d_o	Throttle valve orifice diameter	mm	3.3	3.3
n	Number of throttle valve orifices	-	3	3
C_d	Flow coefficient	-	0.7	0.7
ϵ	Pipe wall roughness	mm	0.046	0.046
p_f	Formation pressure	MPa	4	4, 6, 8, 10

3 RESULTS AND DISCUSSION

3.1 Analysis of the Variation Law of Throttle Valve Pressure Drop with Flow Rate

Based on the specific downhole conditions of Well X in Block X and the established throttle valve pressure drop diversion model, this paper analyzes the influence of fishing fluid flow rate and formation pressure on the pressure drop across the throttle valve. The results in Figs. 8 and 9 reveal a core phenomenon: the pressure drop across the throttle valve is highly sensitive to the fishing fluid flow rate but independent of the formation pressure. The mechanism of this phenomenon stems from the fact that the flow through the throttle valve follows the orifice outflow principle.

As seen in Fig. 8, when the formation pressure is held constant at 4 MPa, the pressure drop across the throttle valve shows a clear nonlinear increase from 1.00 MPa to 5.75 MPa as the fishing fluid flow rate increases from 4 t/h to 10 t/h. The simulation results indicate that the pressure drop is proportional to the square of the fishing fluid flow rate, which is fully consistent with the theoretical prediction of the orifice flow formula. The underlying hydrodynamic mechanism is that the flow through the throttle orifices has entered the turbulent self-similarity regime, and its flow coefficient remains approximately constant within the Reynolds number range studied in this paper ($Re > 10^4$). Consequently, the square relationship between pressure drop and flow rate is established.

Fig. 9 further confirms this mechanism. When the fishing fluid flow rate is kept constant at 6 t/h, despite variations in the downstream formation pressure between 4 and 10 MPa, the pressure drop across the throttle valve remains stable at 2.14 MPa. This is because, according to

mass conservation, changes in formation pressure only slightly adjust the distribution between the flow diverted through the orifices and the flow entering the tubing, but have minimal impact on the key parameter determining the throttle valve pressure drop-the actual flow rate through the orifices. From a hydraulic system perspective, this indicates that the pressure drop characteristic of the throttle valve, as a high local resistance, is essentially decoupled from the resistance of the downstream system. Therefore, in field operations, precise control of the injection flow rate can effectively regulate the throttle valve pressure drop, thereby actively managing the bottom hole pressure.

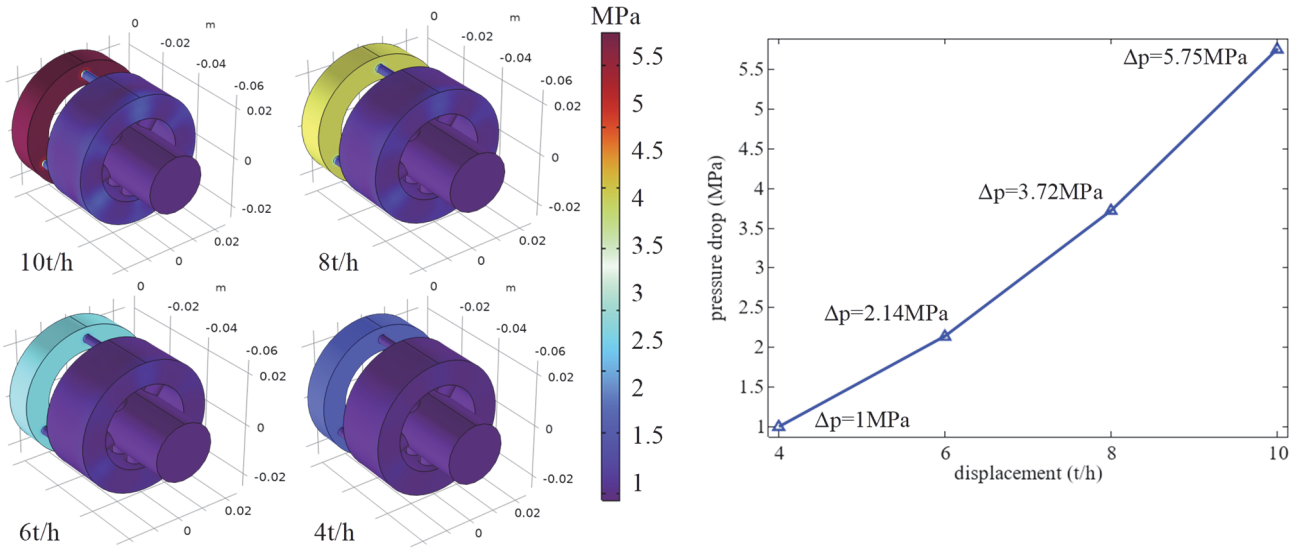

Figure 8 Pressure drop across the throttle valve under different flow rates

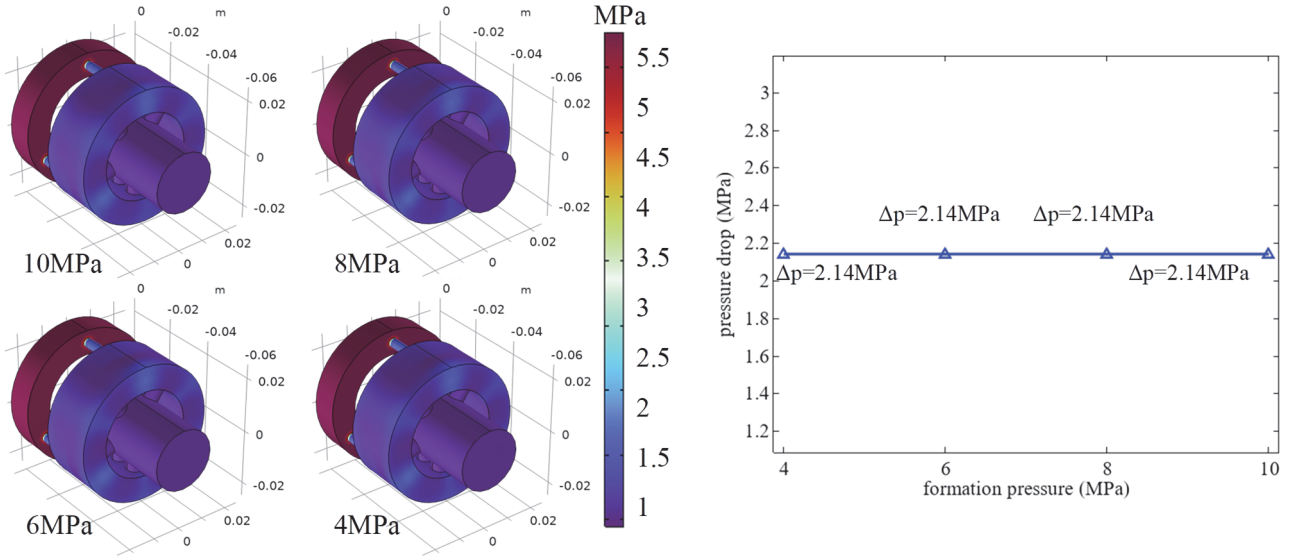

Figure 9 Pressure drop across the throttle valve under different formation pressures

3.2 Analysis of Wellbore Pressure Variation during Fishing Operations

With the introduction of the throttle valve, the wellbore pressure distribution is reconfigured. Based on the pressure drop characteristics of the throttle valve, this paper further analyzes the variation of the full wellbore pressure under the coupled effects of flow rate and formation pressure.

As shown in Fig. 10, the diversion effect of the throttle valve significantly increases the wellhead pressure required for fishing. Taking the formation pressure of 4 MPa as an example, compared to the valve-free condition, the increase in wellhead pressure with the valve rises sharply with increasing flow rate. This increment can be decomposed into two main components: the local pressure drop across the throttle valve and the additional frictional pressure drop due to the increased flow rate in the annulus caused by diversion. At the high flow rate of 10 t/h, the 5.75 MPa local pressure drop across the throttle valve dominates, which directly leads to an equivalent 5.75 MPa increase in the bottomhole annular pressure. Therefore, the nonlinear surge in wellhead pressure is a direct result of the combined action of the valve's local resistance term and the annular friction term. Operationally, the pump injection pressure must be significantly raised according to this nonlinear relationship to maintain the fishing speed.

Fig. 11 reveals another key finding: the influence of formation pressure on the wellhead operating pressure is minimal. At a constant flow rate of 6 t/h, for every 2 MPa increase in formation pressure, the wellhead pressure

increases linearly by only about 0.06 MPa. This can be explained by a series hydraulic resistance model. From the wellhead to the formation, the total pressure drop is consumed by three main parts: annular friction, local resistance of the throttle valve, and tubing friction. Under the conditions of this study, the local resistance of the throttle valve is the dominant resistance. When the formation pressure increases, in order to maintain the same fishing fluid flow rate, the total driving pressure difference remains essentially constant. The increase in formation pressure mainly manifests as an elevation of the tubing outlet pressure and has an extremely small impact on the main components constituting the total pressure drop. This indicates that, in a fishing system equipped with a throttle valve, the wellhead pressure is primarily used to overcome the flow resistance of the wellbore and the valve, rather than directly balancing the formation pressure. Meanwhile, Fig. 11 shows that when the throttle valve is considered, the wellhead pressure is consistently about 2.14 MPa higher than in the valve-free case. This fixed pressure difference is precisely the additional resistance term introduced by the throttle valve. In other words, it needs to balance the formation pressure and additionally provide a fixed pressure drop component generated by the throttle valve, which is flow-rate dependent.

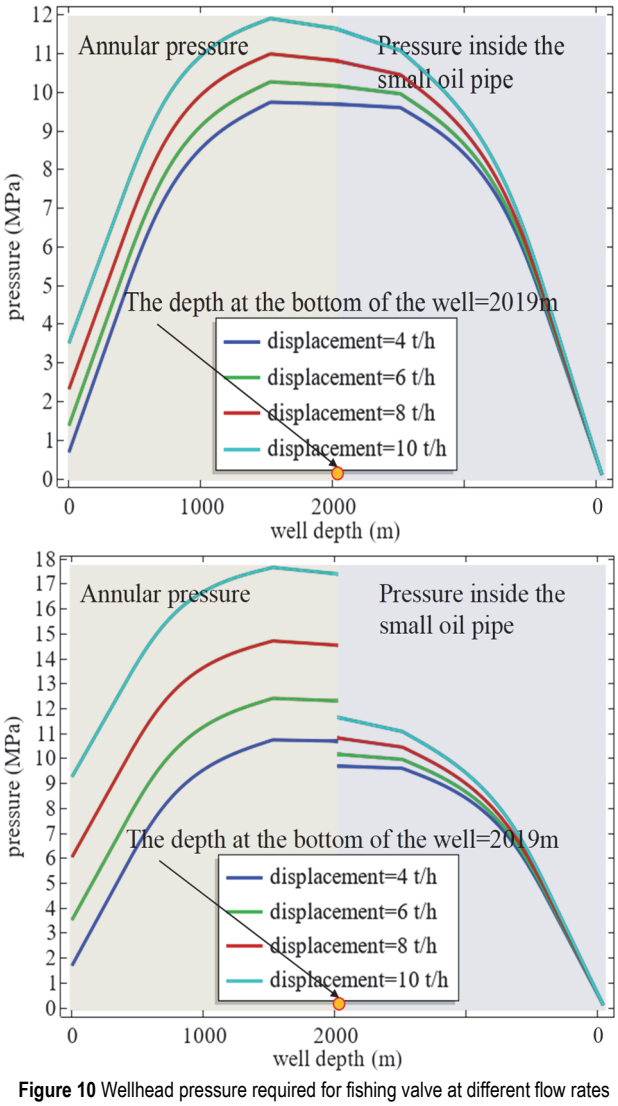

Figure 10 Wellhead pressure required for fishing valve at different flow rates

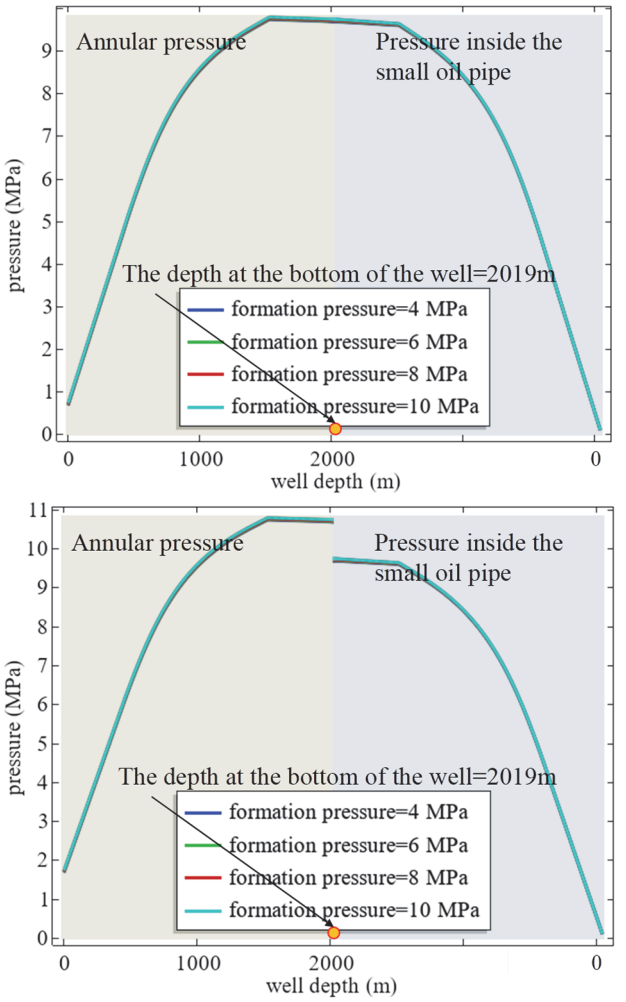

Figure 11 Wellhead pressure required for fishing valve under different formation pressures

4 CONCLUSIONS

This study developed a coupled hydraulic model to characterize the evolution of wellbore pressure during bottom-hole fixed-valve fishing operations in thermal recovery wells. The results indicate that the throttle valve plays a dominant role in wellbore pressure behavior. The pressure drop across the valve is primarily controlled by fluid flow rate and exhibits nonlinear growth, while formation pressure has minimal impact on the overall pressure distribution. The presence of the throttle valve significantly increases both bottomhole and wellhead pressures, highlighting the need for careful management of injection parameters to ensure adequate lifting force for the valve while maintaining a safe operational margin. These findings provide a theoretical basis for optimizing fishing procedures and improving wellbore pressure management strategies in thermal recovery operations. Future work should incorporate multi-well validation, account for transient and multiphase effects, and explore optimization of throttle valve geometries to further enhance prediction accuracy.

5 REFERENCES

[1] Sotoodeh, K. (2021). Subsea valves and actuators: a review of factory acceptance testing (FAT) and recommended improvements to achieve higher reliability. *Life Cycle Reliability and Safety Engineering*, *10*(2), 183-196.

https://doi.org/10.1007/s41872-020-00153-w
[2] Wang, G. (2021). MPD wellbore pressure regulation method based on linear throttle valve. *Oil Drilling & Production Technology*, *43*(2), 197-202. https://doi.org/10.13639/j.odpt.2021.02.010
[3] Li, Y., Si, N., Zhang, T., Liu, M., Yu, L., & Zheng, Y. (2023). Simulation on a new reverse circulation fishing tool: Design and evaluation of the salvage capacity and efficiency. *Energy Science & Engineering*, *11*(6), 2122-2136. https://doi.org/10.1002/ese3.1443
[4] Hu, Y., Li, X. N., Shang, Y. Q., Lu, G. C., Huang, X., & Cui, X. L. (2005). Downhole switch valve for high-temperature wells. *China Petroleum Machinery*, *33*(7), 14-16. https://doi.org/10.3969/j.issn.1001-4578.2005.07.015
[5] Lei, Q., Wang, X., Tang, G., Dong, L., Liao, Y., Feng, X., & Yang, Y. (2020). Simulation and experimental study on fishing performance of vacuum suction wellbore cleaning tool. *Mathematical Problems in Engineering*, *2020*(1), 2371059. https://doi.org/10.1155/2020/2371059
[6] Ahmed, M. A., Hatem, S. M., & Alabdaly, I. K. (2023). Numerical Examination of Heat Transfer and Entropy Generation in Confined-Slot Jet Impingement Featuring Wing Ribs. *Power Engineering and Engineering Thermophysics*, *2*(3), 173-187. https://doi.org/10.56578/peet020305
[7] Laouar, S., Sakib, M. N., Muqit Al, S., Navasardyan, M., & Kutsenko, K. (2020). Pressure drop in valve for different open flow areas. *Journal of Physics: Conference Series*, *1439*(1), 012009. https://doi.org/10.1088/1742-6596/1439/1/012009
[8] Yang, P., Mao, L., Yang, S., & Chen, X. (2025). Research on Wellbore Pressure in the Dynamic Killing Process for Complex Structure Wells Based on the Wellbore Multiphase Flow Theory. *Applied Mathematics and Mechanics*, *46*(2), 254-270. https://doi.org/10.21656/1000-0887.450061
[9] Ouyang, Y., Zhang, G., Huang, H., Li, J., Yang, H., & An, J. (2024). A wellbore multiphase flow model for solid fluidization mining of natural gas hydrate. *China Petroleum Machinery*, *52*(7), 1-9. https://doi.org/10.16082/j.cnki.issn.1001-4578.2024.07.001
[10] Yin, B., Chen, C., Feng, K., Liu, S., Ren, M., Wang, Z., & Sun, B. (2025). Multiphase transient flow in wellbore during shallow hydrate reservoir drilling in deep water. *ACS Omega*, *10(*13), 13701-13714. https://doi.org/10.1021/acsomega.5c01229
[11] Chen, Y., Wang, G., Dong, X., Tang, Y. (2025). Research on linear design of managed pressure drilling throttle valve based on variable-diameter profile optimization. *China Mechanical Engineering*.
[12] Du, J., Liu, H., Wang, J., Xu, X., Wang, Y., Wang, W., Chi, M. (2025). Research and optimization application of throttle erosion laws of electric throttle valve in surface processes of ultra-deep gas wells. *Drilling & Production Technology*, *48*(6), 122-128. https://doi.org/10.3969/J.ISSN.1006-768X.2025.06.15
[13] Qu, G., Li, J., Peng, C., & Guo, Q. (2023). Structure improvement and parameter optimization of micro flow control valve. *Scientific Reports*, *13*(1), 6850. https://doi.org/10.1038/s41598-023-30955-8
[14] Deng, H., Tang, G., & Zhang, L. (2023). Sa study on evolution law of complex flow pressure in ultra-deep wells with high temperature and high pressure. *Journal of Southwest Petroleum University (Science & Technology Edition)*, *45*(4), 111-120. https://doi.org/10.11885/j.issn.1674-5086.2022.09.17.01
[15] Feng, X., Miao, H., Dou, G., Yuan, J., & Yue, C. (2024). Application of coiled tubing fishing technology for complex downhole objects in shale gas horizontal wells. *West-China Exploration Engineering*, *36*(11), 85-88. https://doi.org/10.3969/j.issn.1004-5716.2024.11.023
[16] Gong, W., Li, C., Deng, S., & Ren, Q. (2025). Simulation study on the solid-liquid two-phase flow in the annulus of fishbone-shaped multilateral horizontal wells. *Petroleum Science and Technology*. https://doi.org/10.1080/10916466.2025.2536473
[17] Jafari Raad, S. M., Lawton, D., Maidment, G., & Hassanzadeh, H. (2021). Transient non-isothermal coupled wellbore-reservoir modeling of CO_2 injection: Application to CO_2 injection tests at the CaMI FRS site, Alberta, Canada. *International Journal of Greenhouse Gas Control*, *111*, 103462. https://doi.org/10.1016/j.ijggc.2021.103462
[18] Chauhan, V., Saevarsdottir, G., Tesfahunegn, Y. A., Asbjornsson, E., & Gudjonsdottir, M. (2021). Computational study of two-phase flashing flow in a calcite scaled geothermal wellbore. *Geothermics*, *97*, 102239. https://doi.org/10.1016/j.geothermics.2021.102239
[19] Abdelaal, M. & Zeidouni, M. (2023). Coupled wellbore–reservoir modelling to evaluate CO_2 injection rate distribution over thick multilayer storage zones. *International Journal of Greenhouse Gas Control*, *129*, 103987. https://doi.org/10.1016/j.ijggc.2023.103987
[20] Leporini, M., Terenzi, A., & Marchetti, B. (2021). Improvement of a multiphase flow model for wellhead chokes under critical and subcritical conditions using field data. *Journal of Petroleum Exploration and Production Technology*, *11*, 1487-1503. https://doi.org/10.1007/s13202-021-01114-4
[21] Gabel, T., Mitra, H., Williams, D., Koeck, F., Ostilla-Mónico, R., & Alba, K. (2022). Incompressible flow through choke valve: An experimental and computational investigation. *Journal of Fluids and Structures*, *113*, 103669. https://doi.org/10.1016/j.jfluidstructs.2022.103669
[22] Tellache, N. E., Hassen, M. W., Otmanine, M., & Khodja, M. (2021). Improved multiphase flow rate models for chokes in the Algerian HMD oil field. *Arabian Journal for Science and Engineering*, *46*(7), 6817-6833. https://doi.org/10.1007/s13369-020-04971-z
[23] Alakbari, F. S., Ayoub, M. A., Awad, M. A., Ganat, T., Mohyaldinn, M. E., & Mahmood, S. M. (2025). A robust pressure drop prediction model in vertical multiphase flow: A machine learning approach. *Scientific Reports*, *15*, 13420. https://doi.org/10.1038/s41598-025-98517-4
[24] Akbari, A., Ghazi, F., & Kazemzadeh, Y. (2025). Machine learning-based prediction of well performance parameters for wellhead choke flow optimization. *Scientific Reports*, *15*, 44182. https://doi.org/10.1038/s41598-025-99051-1
[25] Nazari, L. F., Camponogara, E., Imsland, L. S., & Seman, L. O. (2024). Neural networks informed by physics for modeling mass flow rate in a production wellbore. *Engineering Applications of Artificial Intelligence*, *128*, 107528. https://doi.org/10.1016/j.engappai.2023.107528
[26] Wang, X., Huang, L., Li, X., Bi, S., Li, H., Zhang, J., & Sun, X. (2022). Wellbore multiphase flow behaviors of gas kick in deep water horizontal drilling. *Frontiers in Physics*, *10*, 1049547. https://doi.org/10.3389/fphy.2022.1049547
[27] Wang, D. & Zhang, H. (2020). Research on flow characteristics of throttle valve based on fluent. *Journal of Physics: Conference Series*, *1676*(1), 012021. https://doi.org/10.1088/1742-6596/1676/1/012021

Contact information:

Zhuoran LI
(Corresponding author)
Key Laboratory of Enhanced Oil and Gas Recovery of Ministry of Education,
Northeast Petroleum University,
Daqing, Heilongjiang 163318, China
E-mail: 3493076747@qq.com

NOMENCLATURE

p_a	annular pressure, Pa
ρ	fluid density, kg/m³
g	gravitational acceleration, m/s²
f_a	annular friction factor, dimensionless
v_a	annular flow velocity, m/s
$D_{h,a}$	annular Diameter, m
D_c	tubing inner diameter, m
D_o	Coiled Tubing Outer Diameter, m
Re	The Reynolds number, $Re = \frac{\rho v_a D_{h,a}}{\mu}$
q_{orifice}	flow rate through a single orifice, m³/s
C_d	The flow coefficient (dimensionless, typically ranging from 0.6 to 0.8)
A_o	cross-sectional area of a single orifice, m²
d_o	diameter of the orifice, m
Δp_v	pressure drop across the throttle valve, Pa
p_t	pressure in the tubing string, Pa
f_t	friction factor of the tubing string, dimensionless
v_t	flow velocity inside the tubing string, m/s
$D_{i,t}$	inner diameter of the tubing string, m
Q_{inj}	wellhead injection flow rate
Q_{a}	annular flow rate
Q_{tubing}	flow rate entering the tubing
L	axial depth along the wellbore, m
$\frac{\partial(\rho k)}{\partial t}$	unsteady term, representing the rate of change of turbulent kinetic energy per unit volume over time
$\frac{\partial\left(\rho \bar{\mu}_j k\right)}{\partial x_j}$	convection term, representing the net change in turbulent kinetic energy k due to flux through the control volume boundaries
P_k	production term, representing the most significant source of turbulent kinetic energy
$\rho\epsilon$	dissipation term, representing the irreversible conversion rate of turbulent energy into internal energy
$\frac{\partial(\rho\epsilon)}{\partial t}$	unsteady term
$\frac{\partial\left(\rho \bar{u}_j \epsilon\right)}{\partial x_j}$	convection term
$C_{1\epsilon}\frac{\epsilon}{k}P_k$	production term, representing the most significant source of turbulent kinetic energy
$C_{2\epsilon}\rho\frac{\epsilon^2}{k}$	dissipation term, representing the inevitable rate of conversion to internal energy in turbulence.

Greek Symbols

θ	the well deviation angle, °
ϵ	absolute roughness of the pipe wall, m
μ	The dynamic viscosity of the fluid, Pa·s.